RL-TR-92-298
In-House Report
December 1992

DYNAMIC BEHAVIOR OF HELIX INTERACTION CIRCUITS

Peter J. Rocci

APPROVED FOR PUBLIC RELEASE; DISTRIBUTION UNLIMITED.

Rome Laboratory
Air Force Materiel Command
Griffiss Air Force Base, New York

This report has been reviewed by the Rome Laboratory Public Affairs Office (PA) and is releasable to the National Technical Information Service (NTIS). At NTIS it will be releasable to the general public, including foreign nations.

RL-TR-92-298 has been reviewed and is approved for publication.

APPROVED:

ANTHONY J. FEDUCCIA, Chief
Systems Reliability Division
Electromagnetics and Reliability Directorate

FOR THE COMMANDER:

JOHN J. BART, Chief Scientist
Reliability Sciences
Electromagnetics and Reliability Directorate

If your address has changed or if you wish to be removed from the Rome Laboratory mailing list, or if the addressee is no longer employed by your organization, please notify RL (ERSD) Griffiss AFB NY 13441-5700. This will assist us in maintaining a current mailing list.

Do not return copies of this report unless contractual obligations or notices on a specific document require that it be returned.

REPORT DOCUMENTATION PAGE

Form Approved
OMB No. 0704-0188

1. AGENCY USE ONLY (Leave Blank)	2. REPORT DATE	3. REPORT TYPE AND DATES COVERED
	December 1992	In-House Oct 90 - May 92

4. TITLE AND SUBTITLE

DYNAMIC BEHAVIOR OF HELIX INTERACTION CIRCUITS

5. FUNDING NUMBERS

PE: 62702F
PR: 2338
TA: 02
WU: 2U

6. AUTHOR(S)

Peter J. Rocci

7. PERFORMING ORGANIZATION NAME(S) AND ADDRESS(ES)

Rome Laboratory
525 Brooks Road
Griffiss AFB NY 13441-4505

8. PERFORMING ORGANIZATION REPORT NUMBER

RL-TR-92-298

9. SPONSORING/MONITORING AGENCY NAME(S) AND ADDRESS(ES)

10. SPONSORING/MONITORING AGENCY REPORT NUMBER

11. SUPPLEMENTARY NOTES

Rome Laboratory Project Engineer: Peter J. Rocci/ESRD (315)330-4891

12a. DISTRIBUTION/AVAILABILITY STATEMENT

Approved for public release; distribution unlimited.

12b. DISTRIBUTION CODE

13. ABSTRACT (Maximum 200 words)

The dynamic behavior of a high power traveling wave tube's (TWT) helix interaction circuit was determined while operating in its system environment. The purpose of this effort was to develop a fundamental knowledge base of material interactions under thermal loading, develop an understanding of long-term thermal effects on materials and to develop a relationship to TWT performance and reliability. The interaction circuit for the TWT analyzed consists of a variable pitch tungsten helix, three beryllia support rods spaced at equal 120 degree intervals around the helix, and a stainless steel barrel which encloses the vacuum envelope. A three-dimensional finite element model was constructed that represented the entire interaction circuit (8^{1} helix turns in length). There was a great deal of complexity associated with the development of this model due to the irregular "T-shaped" cross-section of the support rods and variation in pitch of the helix. Upon completion, the model contained approximately 18,000 elements and 45,000 nodes.

14. SUBJECT TERMS	15. NUMBER OF PAGES
Microwave Tubes, Finite Element Analysis	44
	16. PRICE CODE

17. SECURITY CLASSIFICATION OF REPORT	18. SECURITY CLASSIFICATION OF THIS PAGE	19. SECURITY CLASSIFICATION OF ABSTRACT	20. LIMITATION OF ABSTRACT
UNCLASSIFIED	UNCLASSIFIED	UNCLASSIFIED	UL

Abstract

The dynamic behavior of a high power traveling wave tube's (TWT) helix interaction circuit was determined while operating in its system environment. The purpose of this effort was to develop a fundamental knowledge base of material interactions under thermal loading, develop an understanding of long-term thermal effects on materials and to develop a relationship to TWT performance and reliability.

The interaction circuit for the TWT analyzed consists of a variable pitch tungsten helix, three beryllia support rods spaced at equal 120 degree intervals around the helix, and a stainless steel barrel which encloses the vacuum envelope. A three-dimensional finite element model was constructed that represented the entire interaction circuit (89 helix turns in length). There was a great deal of complexity associated with the development of this model due to the irregular "T-shaped" cross-section of the support rods and variation in pitch of the helix. Upon completion, the model contained approximately 18,000 elements and 45,000 nodes.

A steady state heat transfer analysis was performed using calculated heat dissipations and boundary temperatures that were obtained from an experiment performed on the TWT by it's manufacturer. Although the absolute amount of power dissipated by the interaction circuit is relatively small compared to the total heat dissipation of the TWT, it is locally concentrated over small areas which creates large heat fluxes. The resulting temperatures from this analysis were then used as loading conditions in a linear static analysis of a smaller model which represents a 12 turn section of the circuit. This section is located approximately half way between the RF input and output and where backward waves reflected from the TWT's output waveguide are attenuated. It was at this attenuation section where the largest temperature gradient was found.

The failure modes investigated in this study were cracking of the helix tape and fracture of the support rods due to excessive thermal stresses. Cracking of the helix tape would cause an open-circuit to occur while fracture of the support rods could cause small mechanical perturbations in the slow wave structure which may reflect the RF signal. Both cases could possibly lead to electrical failure of the TWT. Static stress analysis of the attenuation section indicated that the stress levels in the helix and support rods due to this particular temperature gradient were within acceptable limits and would not fracture if these components were free of initial cracks or flaws. Stresses through the helix were sufficient to nucleate cracks, however the length of these cracks would be very minute and would not affect the useful life of the helix.

The results of this effort have led to a major increase in the fundamental understanding of helix instabilities in current designs and has led to a method for predicting material instabilities within helix interaction circuits for future designs.

PREFACE

The structural reliability of the interaction circuit of a Traveling Wave Tube (TWT) is assessed in this report. This project was part of a FY 91-92 Rome Laboratory effort entitled "EW-TWT Reliability Enhancement" funded by the PRAM office, Wright-Patterson AFB, OH. All work on the interaction circuit analysis was accomplished in-house at Rome Laboratory with the exception of calculation of the circuit's power dissipation, which was performed under contract by Atlantic Research Corporation.

The author wishes to acknowledge Mr. Douglas Holzhauer, Mr. William Bocchi, Mr. Edward Jones and Mr. Clare Thiem, RL/ERSD, for their technical assistance, along with Mr. Mark Stoklosa, RL/ERSD, for his assistance in operating the Silicon Graphics Workstation.

TABLE OF CONTENTS

List Of Figures

List Of Tables

0.0 Executive Summary

The dynamic behavior of a high power traveling wave tube's (TWT) helix interaction circuit was determined while operating in it's system environment. This effort was initiated as part of the AFOSR Task 2305/J9 and the PRAM funded joint program between Warner Robins-Air Logistics Center (WR-ALC) and Rome Laboratory. The purpose of this effort was to develop a fundamental knowledge base of material interactions under thermal loading, develop an understanding of long-term thermal effects on materials and to develop a relationship to TWT performance and reliability.

The physical integrity of a TWT's interaction circuit, also known as a slow wave structure, was investigated. The structure analyzed in this study is from a helix TWT used in an electronic countermeasures (ECM) system. A helix TWT schematic is shown in Figure 1. This structure consists of a rectangular cross-section tungsten helix, three beryllia support rods, and a thin-walled 304 stainless steel barrel which encloses the circuit. A cross-section of the interaction circuit is shown in Figure 2.

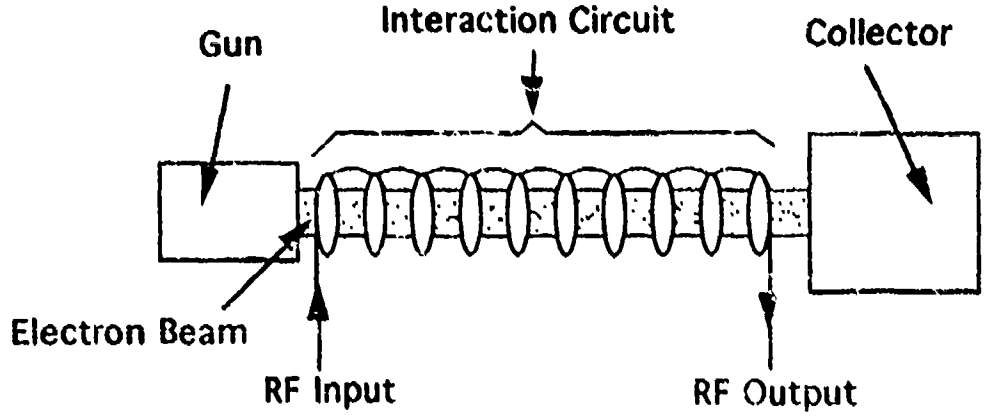

Figure 1: Helix TWT Schematic

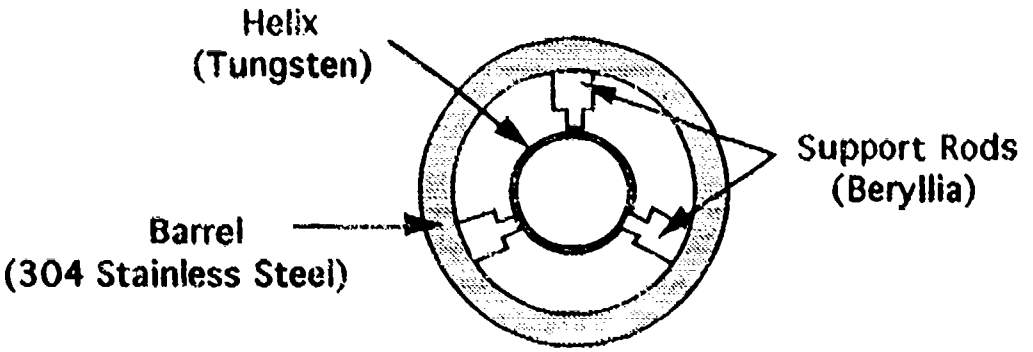

Figure 2: Interaction Circuit Cross-Section

Heat dissipation from ohmic losses and electron beam impingement cause portions of the interaction circuit to experience high operating temperatures that induce material stresses and strains which, if they reach a critical value, can physically damage the interaction circuit. The failure modes investigated in this study were cracking of the helix tape and support rods due to excessive thermal stresses. These failures were analyzed because the mechanical behavior of the helix and support rods under thermal loads is critical to TWT performance. Cracking of the helix tape would cause a short-circuit to occur while cracking of the support rods could cause small mechanical perturbations in the slow wave structure which may reflect the RF signal. Both cases could lead to electrical failure of the TWT.

Finite element techniques were used to determine the structure's steady state thermal response to combined forward and reflected power dissipations and measured boundary temperatures. A three-dimensional finite element model was constructed of the entire interaction circuit (89 helix turns) and a steady state heat transfer analysis was performed using calculated heat dissipations and boundary temperatures obtained from an experiment performed by the TWT's manufacturer. The finite element model contained approximately 18,000 elements and 45,000 nodes. Because of the size of this model, a stress analysis, which involves more degrees of freedom than a thermal analysis and therefore requires a much greater amount of computer memory, could not be performed on the entire

circuit. Therefore, a linear static stress analysis was performed over a smaller portion (12 helix turns in length) of the circuit using the resulting temperatures from the steady state thermal analysis. This section is located approximately half way between the RF input and output and where backward waves reflected from the TWT's output waveguide are attenuated. It was at this attenuation section where the largest temperature gradient was found.

The results of this study show that the stress levels in the helix and support rods were within acceptable limits when the TWT is operating under full forward power and 1000 watts reflected power. This is considered a "worst case" scenario since 1000 watts is the maximum reflected power that this TWT can dissipate (from the TWT's Spare Specification). Mechanical failure would not occur if the helix and rods were free of initial cracks or flaws. The stress levels through the helix were found to be high enough to nucleate small cracks. However, because these cracks would be microscopic in length, the useful life of the helix would probably not be affected.

Finite element analysis can prove to be a valuable tool in advancing TWT technology by aiding in the design of future TWT components. Up-front structural reliability assessments can be made on a component before production actually begins to insure that it can withstand conditions it was designed for. Finite element can also be used as an analysis tool for identifying design flaws in previously failed tubes and assist in the diagnostics associated with forensic analysis of these tubes. The results of this effort have led to a major increase in the fundamental understanding of helix instabilities in current designs and has led to a method for predicting material instabilities within helix interaction circuits for future designs.

All work on this project was conducted in-house at Rome Laboratory. The finite element analyses were performed on the System Reliability & Engineering Division's Silicon Graphics 210GTX workstation using NISA, a commercially available finite code developed by Engineering Mechanics Research Corporation (EMRC).

1.0 Introduction

The unique combination of bandwidth and gain provided by TWT's has yet to be matched by any other device. The operation of a TWT depends on the continuous interaction of a beam of electrons with an electromagnetic wave. The interaction circuit analyzed in this study is from a helix TWT used in an electronic countermeasures (ECM) system. The circuit employs a rectangular cross-section helix tape which a radio frequency (RF) signal is propagated down at a speed near that of light. However, the axial velocity of the wave is reduced by the pitch of the helix. When an electron beam is injected along the axis of the helix, the axial electric field accelerate some electrons and decelerate others [7]. This causes electrons in the beam to form "bunches" which interact with the helix RF wave, surrendering energy to it. By the time the RF signal reaches the output coupler, it has been amplified exponentially.

The helix from this TWT is constructed of tungsten, has a rectangular cross-section and variable pitch. Tungsten is an attractive material for high temperature applications because of it's extremely high melting point (≈ 3400 degrees C), and high ductile-brittle transition temperature. Three dielectric support rods equispaced around the helix act to hold the helix in place and also provide a path by which heat is removed from the helix. These rods also attenuate any backward wave which reflects from the output waveguide back through the circuit. Beryllia is used because of it's good thermal conductivity at high temperatures and ease of fabrication. The rods are coated with a thin film of carbon over a length of about twenty helix turns starting approximately half way between the RF input and RF output. This carbon coating dissipates any reflected waves in the form of heat. The helix and support rods are enclosed in a vacuum environment by a thin-wall barrel constructed of 304 stainless steel.

When the TWT is powered up, heating of the helix occurs from heat dissipations due to ohmic losses and electron beam impingement. The dielectric support rods also dissipate heat, partially from ohmic losses associated with the forward wave but mostly from fully dissipating any reverse waves that reflect back through the circuit from the output

coupler. These heat dissipations induce a temperature distribution through the circuit, which in turn, induces a thermal stress distribution. If stresses reach a critical value, cracking of the helix tape and/or support rods can occur, which could lead to electrical failure of the TWT. Whether or not these thermal stresses lie within the region of safe operation is a good indication of the interaction circuit's structural reliability.

MIL-HDBK-217, Reliability Prediction of Military Equipment, provides a model to predict operating failure rates for Traveling Wave Tubes based on tube characteristics and operating environment. This model was formulated from failure data obtained from previously designed tubes and only considers the reliability of the overall TWT. Since, no mathematical model exists that can be used to predict the reliability of critical TWT components, finite element techniques were used to determine the circuit's thermal/mechanical performance and the results used to assess the circuit's structural integrity.

The FEA code used at Rome Laboratory is Numerically Integrated Elements for System Analysis (NISA). NISA's steady state heat transfer code was used to simulate the circuit's response to a constant heat load and previously measured boundary temperatures. The resulting temperature distribution was used as a thermal load into NISA's static stress code. Results from the stress analysis were then used with the maximum normal stress theory to determine if the calculated stress levels were high enough to cause failure of the helix and support rods. Fracture mechanism maps were then used to determine the fracture behavior for both tungsten and beryllia. These maps take into account the temperatures and stresses experienced by these materials as well as the presence of pre-existing cracks or flaws.

This report is organized in the following manner. First, the method of construction of the finite element model is described and attributes of this model are defined. Next, all input variables associated with the steady state thermal analysis are described and results of this analysis are presented. These results are then input into the stress analysis code and resulting stresses are presented. Finally, these results are interpreted using appropriate material failure and fracture theories.

2.0 Finite Element Model

Finite element models are numerical models that represent an actual physical system. The three-dimensional finite element developed for this study is shown in Figure 3. A 3-D model was constructed because it was felt that the heat flow through this structure would not be restricted to two dimensions. The model was constructed interactively using NISA's DISPLAY pre-processor. Figure 3 shows a portion (≈ 35 %) of the model used in the heat transfer analysis. The whole model consists of 89 helix turns, support rods and vacuum envelope barrel. It contains approximately 18,000 elements and 45,000 nodes.

Before elements and nodes were generated, the structure's geometry had to be defined. Because of the irregular geometries associated with this structure, the geometry definition was not a trivial task. The first entity that was created was the helix tape. DISPLAY allows the user to create helix curves by defining the curve's center line, radius, pitch and total length. Eighty-nine of these curves were generated which represents the entire length of the helix. The variable pitch of the helix was also accounted for when generating these curves. The curves were then "dragged" into a second, then a third dimension, representing a 3-D, rectangular cross-section helix tape. Next, the support rods were created. Because of the irregular "T-shaped" cross-section and curved surfaces associated with these rods, this was a complex geometry to define. Through manipulation of several grid points and lines, individual 3-D rod sections were created on each turn of the helix at 120 degree intervals. Using NISA's "Macro" utility, this process was repeated over all 89 helix turns. A Macro is a set of user input commands that control the production and execution of DISPLAY command lines. This particular Macro contained all of the necessary commands to construct a 3-D rod section on the surface of the helix and the control structure which, when read in by DISPLAY executed these commands a specified amount of times. Since there were 267 rod sections to be created (3 rod sections/helix turn x 89 helix turns = 267 rod sections), use of this utility saved an enormous amount of time. Using a second Macro algorithm, the spaces in between the helix turns were filled in, resulting in three continuous support rods equispaced at

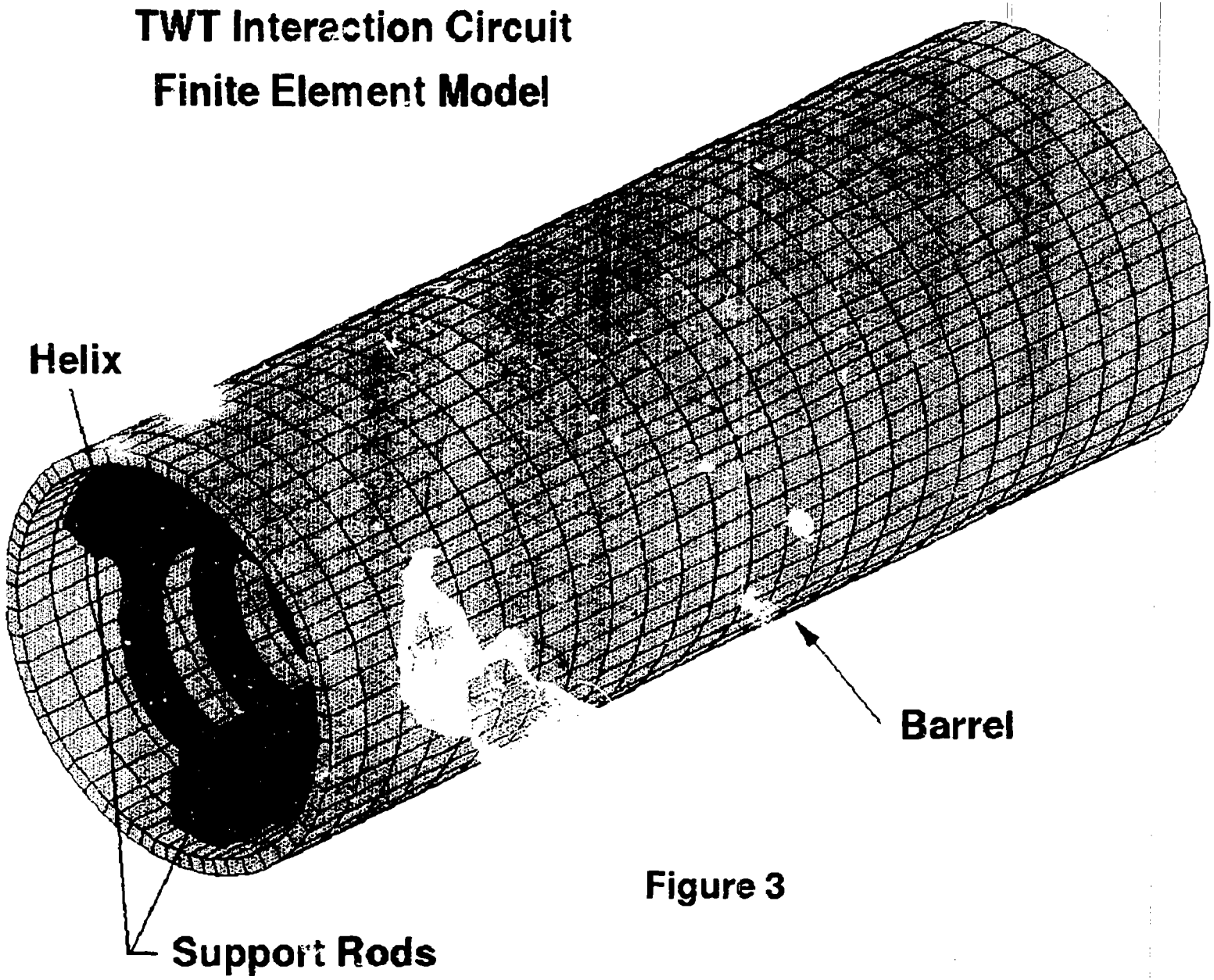
TWT Interaction Circuit
Finite Element Model
Helix
Barrel
Support Rods

Figure 3

120 degree intervals around the helix. Finally, the vacuum envelope barrel was easily defined by creating a hollow cylinder with the appropriate outside diameter, thickness and length.

After the entire geometry was defined, finite elements were generated. The element type used for the heat transfer analysis was NISA type 104, a 3-D solid, hexahedron (brick) element suited for modeling 3-D heat flow (Figure 4). This element contains eight nodes, one per corner. For the static stress analysis, NISA element type 4 was employed. This element is based on a 3-D state of stress and is suited for modeling 3-D solids subject to 3-D loading. These two element types are identical in shape and orientation with their only difference being that type 104 has one degree of freedom per node (temperature), while type 4 has three degrees of freedom per node (x, y and z translations).

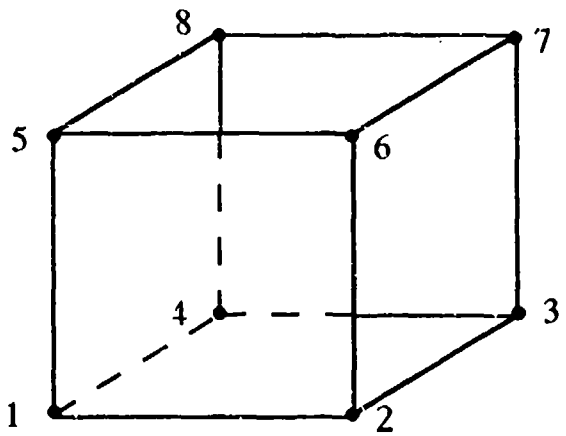

Figure 4: 3-D, 8-Noded Hexahedron (Brick) Element

3.0 Steady State Heat Transfer Analysis

The steady state heat transfer analysis performed in this study simulated the interaction circuit's thermal performance under constant (non-time-dependent) heat dissipations and boundary temperatures. Generally, the typical temperature differences between the helix and the cooling jacket are such that the effect of radiation from the helix can be neglected and, with the helix in a vacuum environment, there is no convection [4]. Therefore, we can assume that heat is transferred only by conduction from the helix, through the support rods, out through the barrel, which encloses the vacuum envelope.

Heat Dissipation

The interaction between the dc electron beam and RF wave is the most complicated process in the TWT. In calculating the heat dissipations through the interaction circuit, a modeling approach was adopted to work backwards from a given TWT RF output power and forwards from a given RF input power to determine an "effective" TWT gain parameter for the forward wave and an "effective" attenuation parameter for the reflected wave. To simplify this procedure, the following assumptions were made.

1. The interaction structure was modeled as a lossy coaxial transmission line. Ohmic losses are assumed to occur on both the helix and inner surface of the barrel.

2. The regions of the dielectric support rods which contain the attenuation coating partially dissipate the forward power and fully dissipate the reflected power.

3. The forward power gain is an exponential function of the interaction length.

4. TWT operation occurs in the small signal region only.

From the spare specification for this particular TWT, the following information was used in calculating heat dissipations.

1. Maximum input Voltage Standing Wave Ratio (VSWR) =2.5:1

2. Maximum output VSWR = 2.7:1

3. Maximum return power from output = 1000 watts

Using the aforementioned facts and assumptions, heat dissipations through the circuit were calculated for forward, reverse, and combined forward/reverse power. The values for combined forward/reverse power were used as inputs to the finite element model because it was felt that this would represent a "worst case" heat dissipation. Also, since the heat dissipated at the surface of the barrel was an order of magnitude less than the heat dissipated by the helix, it would have little or no effect on the overall temperature distribution and therefore was not included in this analysis. Heat generation was simulated on the inside surface of the helix, which represented most of the forward wave loss, and on the attenuation portion of the dielectric support rods, which accounts for a small percentage of the forward wave loss and the entire reflected wave loss.

Boundary Temperatures

In order to provide a path for the heat to flow, boundary temperatures were designated over the entire outside surface of the barrel. The manufacturer of this particular TWT ran a test on the same band TWT which provided Rome Laboratory with realistic boundary temperatures. The TWT was first stripped down to the barrel and modified to route three thermocouple wires. Three thermocouples were then spotwelded to the barrel. The TWT was then re-assembled, the gun re-potted, and the test was performed. Temperatures were recorded at several operating frequencies under each of the following conditions.

1. Ambient oil (75 degrees C), RF at low drive.

2. Ambient oil, RF at saturated output power.

3. Hot oil (100 degrees C), RF at low drive.

4. Hot oil, RF at saturated output power.

5. Ambient oil, 2:1 VSWR mismatch on output, RF at low drive.

6. Ambient oil, 2:1 VSWR, RF at saturated output power.

7. Hot oil, 2:1 VSWR, RF at low drive.

8. Hot oil, 2:1 VSWR, RF at saturated output power.

The case which most closely represented the conditions under which the heat dissipations were calculated, as well as a worst case condition was hot oil, 2:1 VSWR mismatch and RF at saturation. Using temperature values at the same frequency for which heat dissipations were calculated, temperatures were assigned at each node on the outside surface of the barrel. Linear interpolation was used to determine temperatures at node points that lie in between the thermocouple coordinates and it was assumed that these temperatures remained constant around the circumference of the barrel.

Coupled Nodes

To account for the helix-rods and rods-barrel conduction path, appropriate nodes on these structures were thermally coupled, that is, forced to exist at the same temperature. This coupling of nodes causes the calculated helix temperatures to be lower than the actual temperatures because the thermal interface resistances for the helix-rods and rods-barrel interfaces are not accounted for. These thermal resistances are a function of the contact pressures between the components, since there are no bonding materials, brazes or welds associated with the structure. This data was not available for this particular TWT, therefore the thermal resistances could not be determined. Coupling of these nodes, however, would not effect the determination of temperature trends through the interaction circuit, which is the main objective of the thermal analysis.

Material Properties

Each element within the model is defined by a material index number. Each index number has specific material properties associated with it. For a steady state conduction heat transfer analysis, thermal conductivity is the material property that needs to be entered into the input file. NISA has the capability to handle temperature and/or time dependent material properties as well as directional dependent (anisotropic) material properties. For this analysis, all thermal conductivities were assumed to independent of crystallographic direction (isotropic) and independent of time. The thermal conductivities of all three materials were, however, temperature dependent. The nature of this dependency is illustrated in the temperature vs. thermal conductivity graph in Figure 5 [10]. Each data point shown in Figure 5 was entered into the NISA input file. The NISA code interpolated between these points to determine a material's thermal conductivity at any temperature.

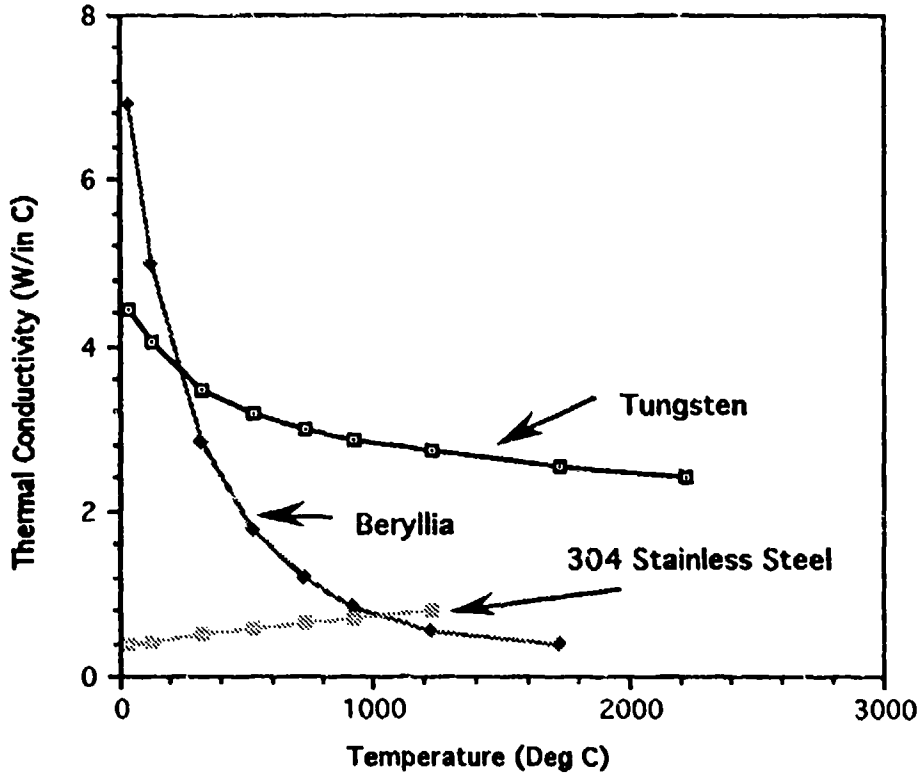

Figure 5: Material Thermal Conductivities

Results

NISA's steady state heat transfer was executed using all of the aforementioned input data. Temperature contours are shown in Figure 6. What can be ascertained from this plot are the specified boundary temperatures on the outer surface of the barrel. Figures 7 and 8 show temperature contours through the helix and support rods for the end and attenuation sections, respectively. These three contour plots indicate the interaction circuit's temperature distribution for combined forward/reverse power under prescribed boundary conditions. The TWT's manufacturer indicated that these temperatures are a good lower bound for the problem but the maximum temperatures should be about 30% higher than the maximum temperatures determined in this analysis. This discrepancy was due to not accounting for the thermal interface resistances between the helix-rods and rods-barrel. These resistances are dependent upon the contact pressures between the components and could not be determined because of lack of information concerning the assembly process of this interaction circuit. This analysis does however, represent a valid description of the temperature trends throughout the circuit.

Steady State Thermal Contours - Entire Model

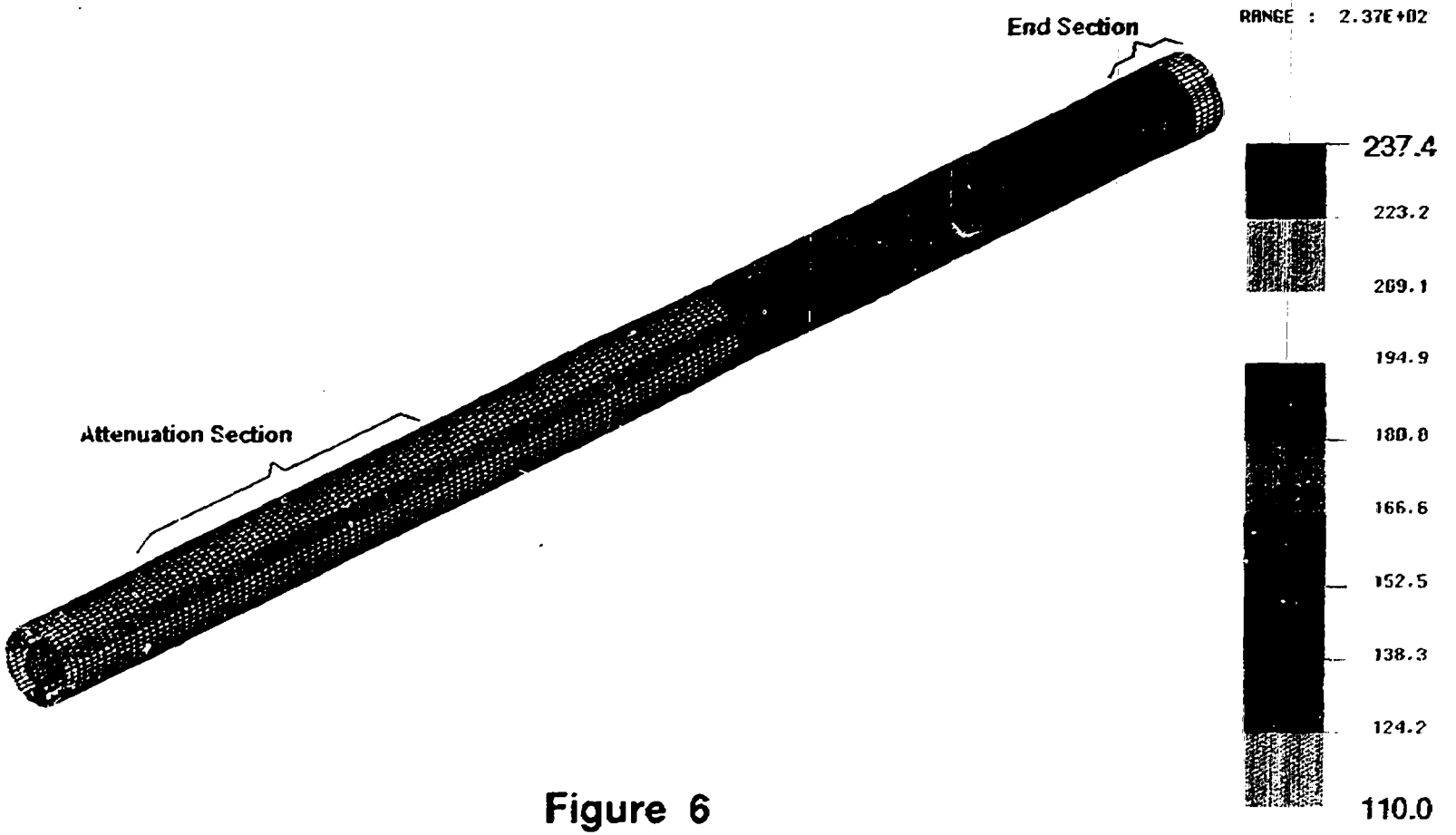

Figure 6

Note: All Temperatures in Degrees C

Steady State Thermal Contours - End Section

(Helix and Support Rods Only)

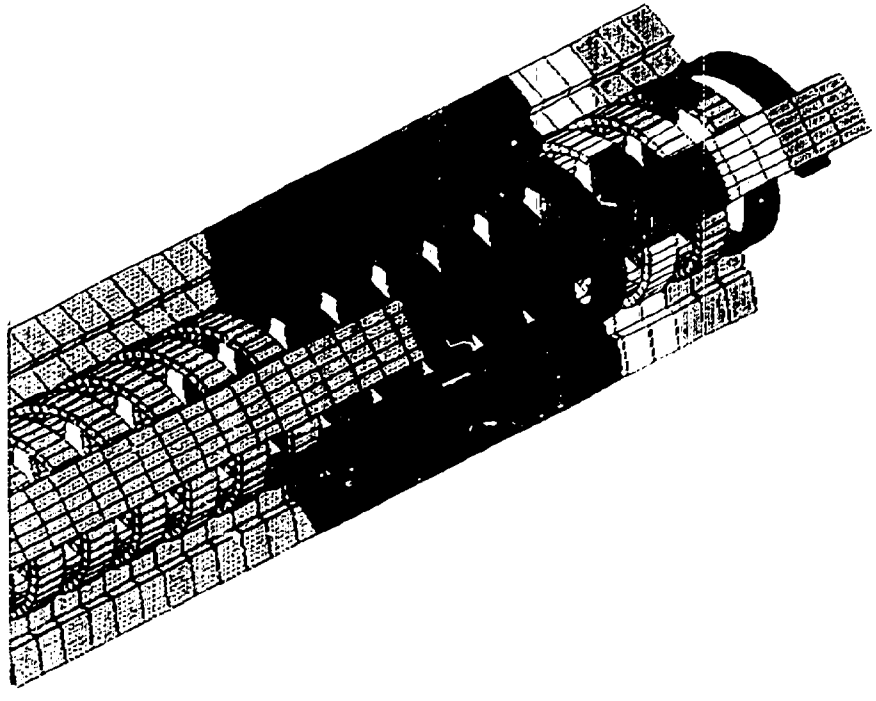

Figure 7

Steady State Thermal Contours - Attenuation Section
(Helix and Support Rods Only)

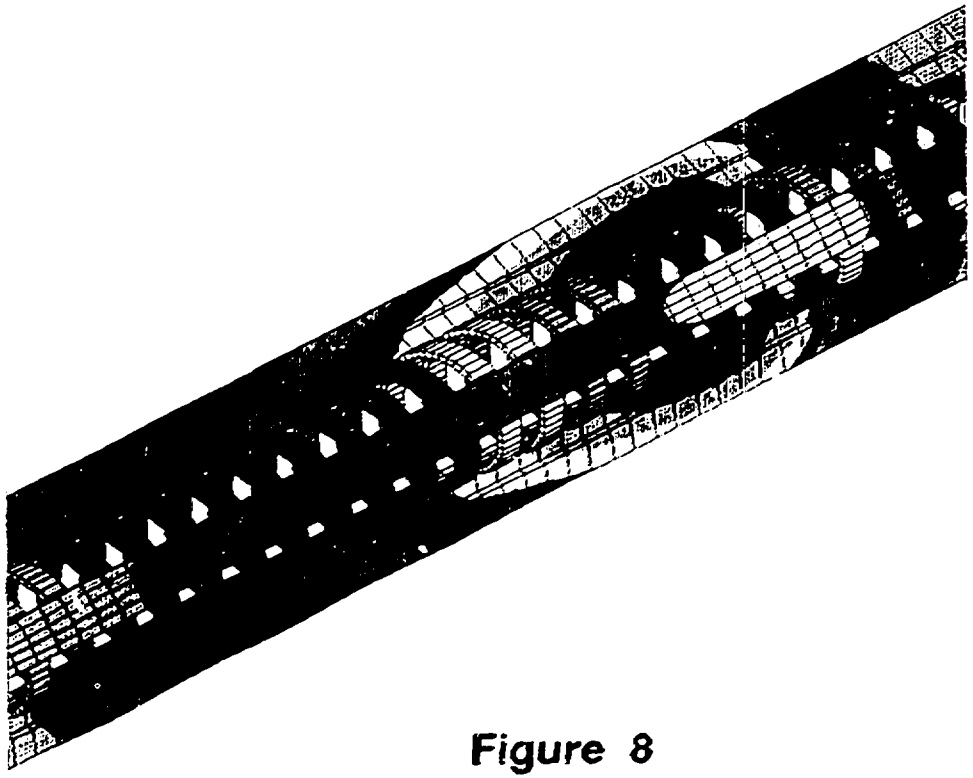

Figure 8

4.0 Thermal Stress Analysis

Thermal stresses are stresses arising from deformations caused by temperature gradients present within a material. When a material is subject to a temperature gradient, the various fibers that make up the material tend to expand (or contract) different amounts. If the material is physically constrained, tensile and/or compressive stresses are induced. When stresses exceed a prescribed level (dependent upon the material), yielding or fracture occurs.

Since the size of the finite element model used in the heat transfer analysis was very large, a stress analysis, which involves more degrees of freedom than does a heat transfer analysis and therefore requires a much greater amount of computer memory, could not be performed on the entire circuit. A smaller portion of the interaction circuit (12 helix turns in length) was therefore selected to perform a linear static stress analysis. This section corresponds to the attenuation section of the circuit where the largest temperature gradient was found, and therefore is the location where the highest thermal stresses will occur. This smaller model consisted of 2,578 elements and 6,476 nodes.

Thermal Loading

The results of the NISA steady state heat transfer analysis gave temperature values at each node within the model. The calculated nodal temperatures were written to an output text file. A FORTRAN 77 program was written that read in this file and wrote a revised text file that contained temperatures only for those nodes present in the attenuation section finite element model. This updated file was then used as a thermal loading condition for the subsequent stress analysis.

Boundary Conditions

In order to apply proper physical constraints to this model, the coordinate system in which the nodal coordinates were defined had to be converted from cartesian to cylindrical (see Figure 9). This was easily accomplished within NISA's pre-processor. Definition of nodal constraints

in the cartesian coordinate system would have led to an invalid stress solution.

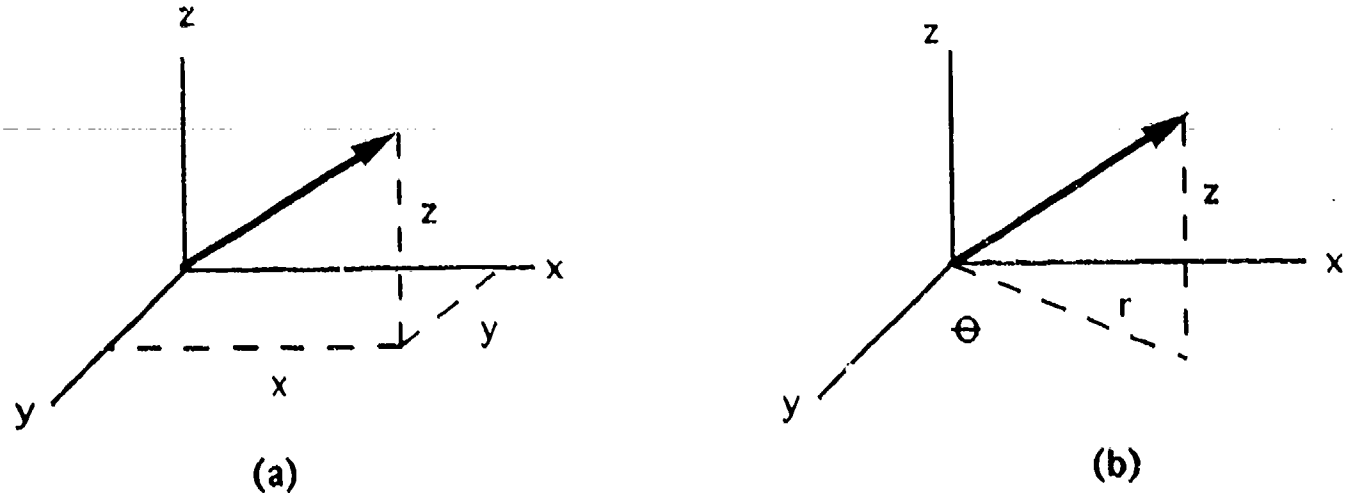

Figure 9: (a) Cartesian and (b) Cylindrical Coordinate Systems

When constraining a finite element model, one must be careful not to overconstrain or inadequately constrain the model since numerical inaccuracies would result. Constraints must be placed on all degrees of freedom associated with the model. If the model were allowed unlimited displacement in any direction, an incomplete solution would arise. When applying these boundary conditions, precautions were taken not to overconstrain the model and to apply proper, realistic displacement constraints.

Figure 10 illustrates the displacement constraints that were placed upon the finite element model. First, all barrel and rod nodes lying on the z=0 plane were constrained in the z-direction (axial direction). Movement in the axial direction was permitted for all remaining nodes. Secondly, a strip of nodes lying along the axial length of the barrel were constrained in the radial direction. Movement in the radial direction was permitted for the remaining nodes. Finally, as a rotational constraint, one node lying on the outside surface of the barrel was constrained, rotation for remaining nodes was permitted.

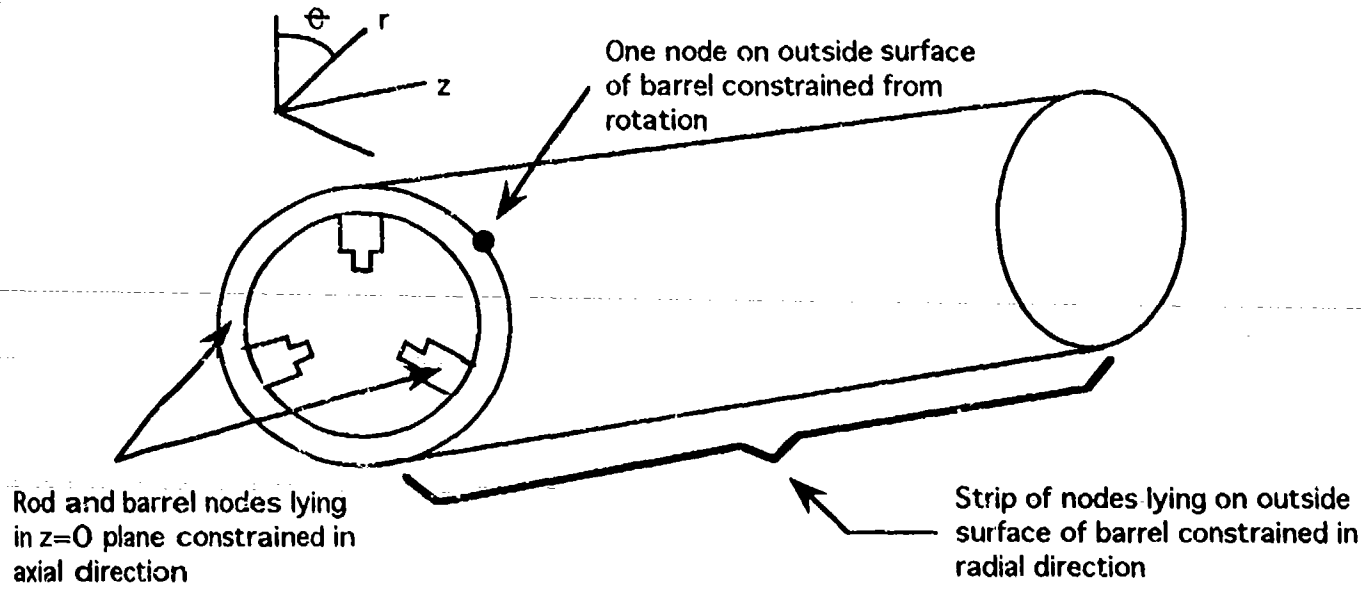

Figure 10: Constraints For Stress Analysis

To account for interfaces between the interaction circuit components, appropriate nodes lying on the helix-rods and rods-barrel interface were coupled together. These nodes were coupled in the radial direction only. This allowed the nodes to move relative to each other in the rotational and axial directions.

Material Properties

The material properties necessary for the stress analysis are shown in Table 1 [1,4,12]. It was assumed that all materials exhibited isotropic behavior. All properties exhibited little or no change with increasing temperature with the exception of the thermal expansion coefficient for tungsten.

	Modulus of Elasticity ($\times 10^6$ psi)	Poisson's Ratio	Density (lb/in^3)	Thermal Expansion Coefficient ($\times 10^{-6}$/C)
Tungster	50.0	.28	.697	4.44 @ 25 C 4.48 @ 150 C 4.55 @ 300 C
Beryllia	48.0	.23	.105	8.0
304 Stainless Steel	29.0	.30	.286	1.7

Table 1: Mechanical Properties

Results

At the onset of this study, the failure modes to be investigated in this study were cracking of the tungsten helix and beryllia support rods. Since there have been no documented TWT failures due to failure of the barrel, stresses through the barrel were ignored.

Before any failure theory could be selected to determine of the calculated stress levels would cause failure, the mechanical behavior of tungsten and beryllia in the operating temperature range had to be identified. Beryllia, a ceramic material exhibits brittle behavior as do most ceramic materials. Tungsten, a metal, exhibits ductile behavior at very high temperatures. However, for temperatures below 1000 degrees C, tungsten behaves in a brittle manner [4,12].

For isotropic materials that fail by brittle fracture, the maximum normal stress theory is the best theory to use [5]. For a triaxial state of stress, the maximum normal stress theory is shown graphically in Figure 11.

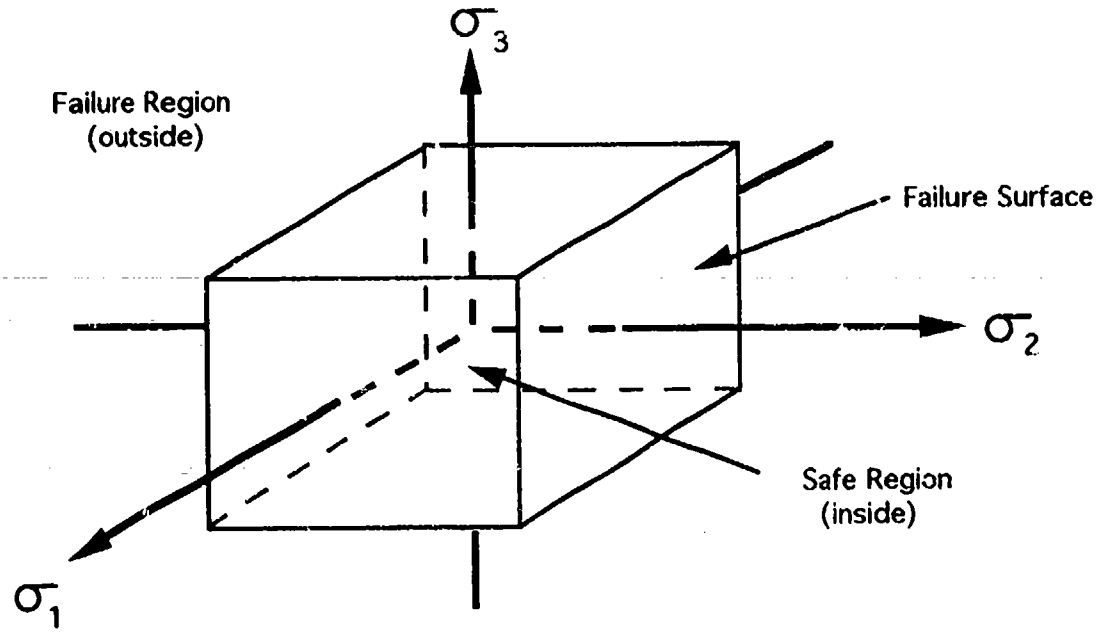

Figure 11: Graphical Representation of Maximum Normal Stress Theory

The surfaces of the cube represent failure surfaces. All states of stress that lie outside the cube would result in failure and all states of stress that lie within the cube would safely tolerate the applied loads without failure. The stresses shown in Figure 11 represent principal stresses. Principal stresses are normal stresses associated with axes on whose normal planes there exists maximum normal stress and zero shear stress. These stresses are ordered such that s_1 (maximum normal tensile stress) is the algebraic maximum and s_3 is the algebraic minimum (maximum normal compressive stress). Therefore, according to this theory, failure will occur in tension if the maximum normal tensile stress (s_1) exceeds the material's ultimate tensile strength, and failure in compression will occur if the maximum normal compressive stress (s_3) exceeds the material's ultimate compressive strength.

Stress contours through the helix and support rods are shown in Figures 12 and 13. The contours shown in Figure 12 are maximum principal stresses (maximum normal tensile stresses), while Figure 13 shows minimum principal stress (maximum normal compressive stress) contours. These results are summarized in Table 2.

Maximum Principal Stresses
Attenuation Section

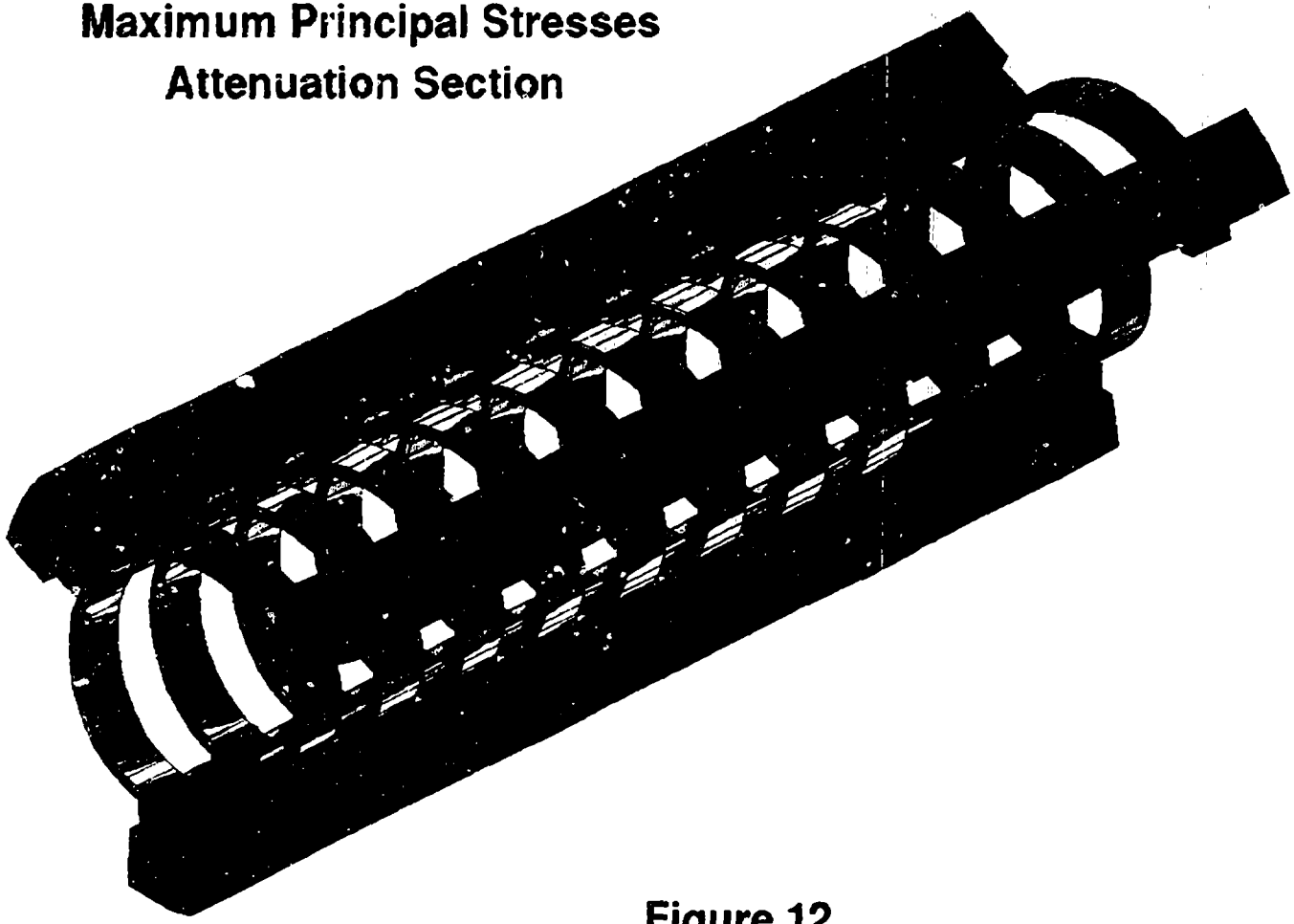

Figure 12

Note: Units in lb/in^2 (psi)

Minimum Principal Stresses
Attenuation Section

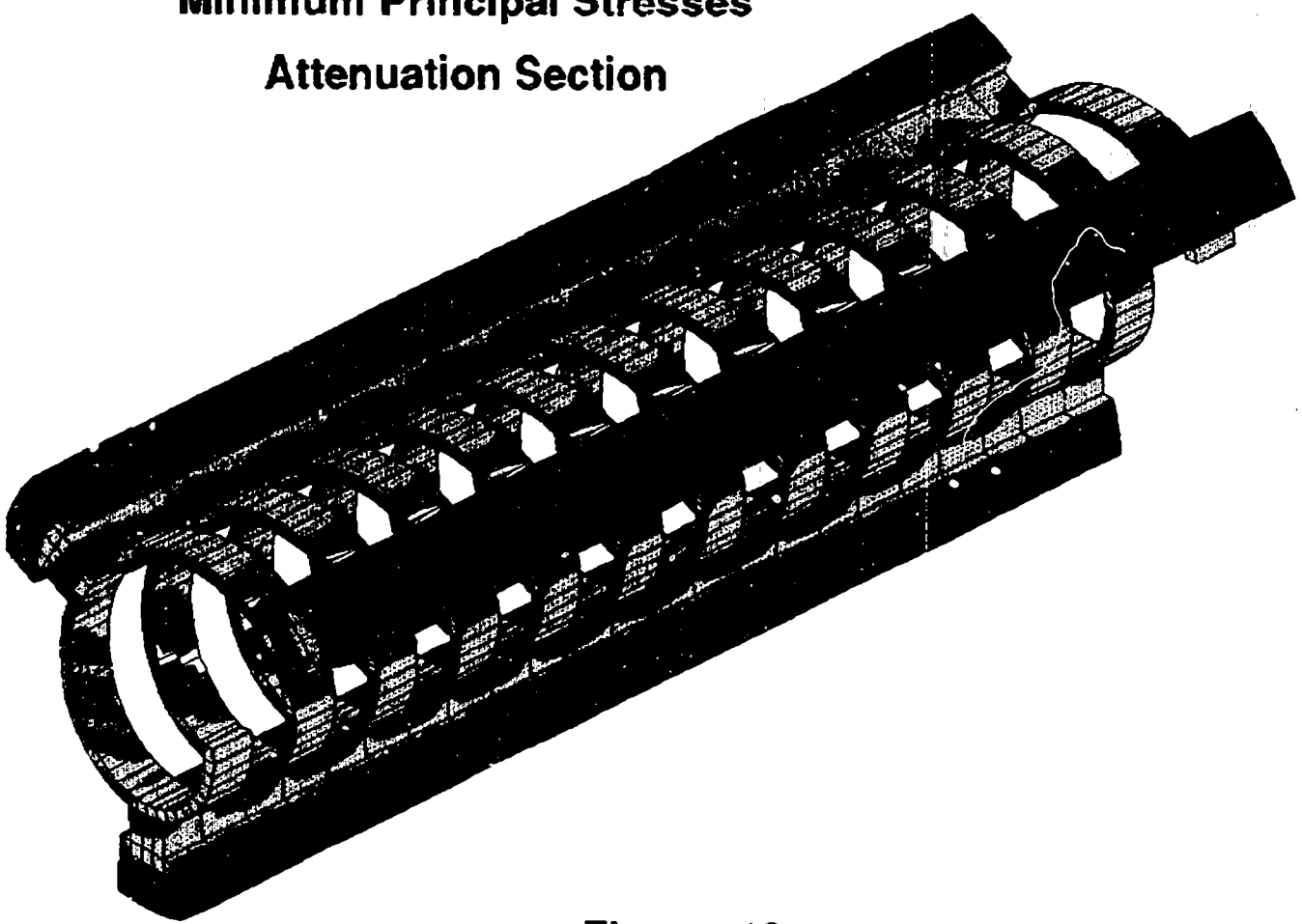

Figure 13

Note: Units in psi

	σ_1 (Maximum Principal Stress) ksi	σ_3 (Minimum Principal Stress) ksi
Helix	79.7	102.6
Support Rods	13.92	43.6

Table 2: Extreme Component Stresses (1 ksi = 1000 psi)

The ultimate tensile and compressive strengths for tungsten and beryllia are given below [1,4,12] :

Tungsten: Ultimate tensile strength ≈ 198-215 ksi
Ultimate compressive strength ≈ 186-210 ksi

Beryllia: Ultimate tensile strength ≈ 23 ksi
Ultimate compressive strength ≈ 18,800 ksi

The maximum normal tensile and compressive stresses through the helix and support rods given in Table 2 lie within the safe range specified by the maximum normal stress theory. Therefore, according to this theory, and the fact that brittle materials do not experience fatigue failure due to accumulation of damage, it can be concluded that mechanical failure of the helix and support rods will not occur when the TWT is operating at full forward power and 1000 watts reflected power.

Fracture Analysis

The fracture behavior of a structure depends on several factors. Stress level, material properties, type of fracture mechanism and presence of pre-existing flaws all impact fracture behavior. If a pre-existing crack or flaw is present, failure can occur over a period of time even if the overall component stress is below it's critical failure stress. For a crystalline solid loaded in tension, several fracture mechanisms exist. However, for

materials that exhibit brittle behavior at sufficiently low temperatures, fracture occurs by cleavage and brittle intergranular fracture [2].

The fracture behavior for tungsten and beryllia was obtained through the use of fracture mechanism maps. These maps are shown in Figures 14 and 15 for tungsten and alumina, respectively [2]. The fracture mechanism map for alumina is typical of the maps for many oxides, and therefore was used to analyze beryllia's fracture behavior. The ordinate on these maps is the material's homologous temperature (T/T_m). T represents the material's temperature and T_m the material's melting point. From the temperatures determined in the steady state heat transfer analysis, T/T_m for both tungsten and beryllia is approximately 0.1. The abscissa on these maps is the normalized tensile stress, which is defined as the maximum normal tensile stress (Table 2) divided by the elastic modulus (both of these variables are dimensionless). Since T/T_m for both materials is around 0.1, the only fracture mechanisms present will be Cleavage 1 and Cleavage 2. Cleavage 1 occurs when pre-existing cracks or flaws are present which can propagate at stresses below the critical failure stress. When a crack reaches a critical length, fracture occurs. If pre-existing cracks or flaws are small or absent, stresses can reach a level which can nucleate cracks. This regime of nucleation of cracks is called Cleavage 2.

For tungsten, the normalized tensile stress was calculated to be .00159. The point (0.1,.00159) in Figure 14 lies on the boundary between Cleavage 1 and Cleavage 2. This indicates that fracture can occur if there are pre-existing cracks or flaws and it is possible for cracks to nucleate if pre-existing cracks or flaws are small or absent. The normalized tensile stress for beryllia was calculated to be .00029. The point (0.1,.00029) in Figure 15 lies within the Cleavage 1 regime. Therefore, if there are no pre-existing cracks or flaws present, fracture of the support rods will not occur.

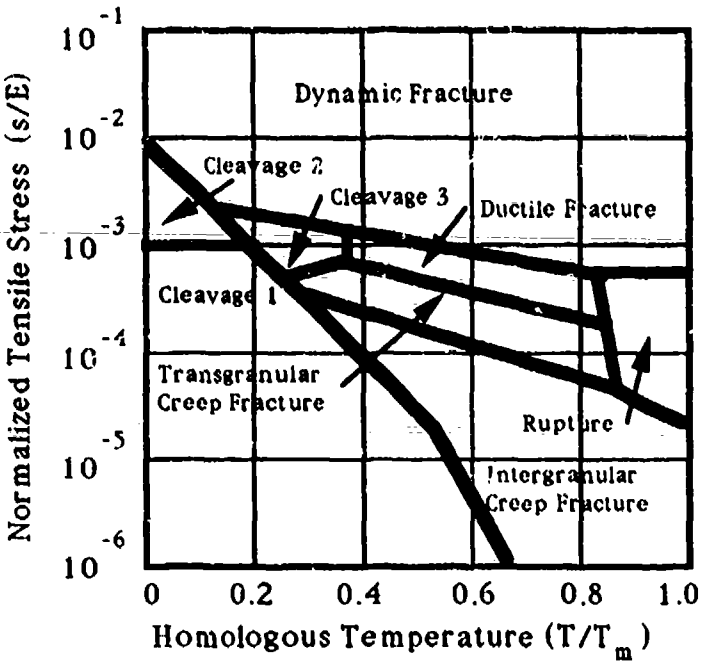

Figure 14: Fracture Mechanism Map For Tungsten

(From Ashby, M.F., *Micromechanisms of Fracture in Static and Cyclic Failure*, Fracture Mechanics - Current Status, Future Prospects, Pergamon Press, 1979)

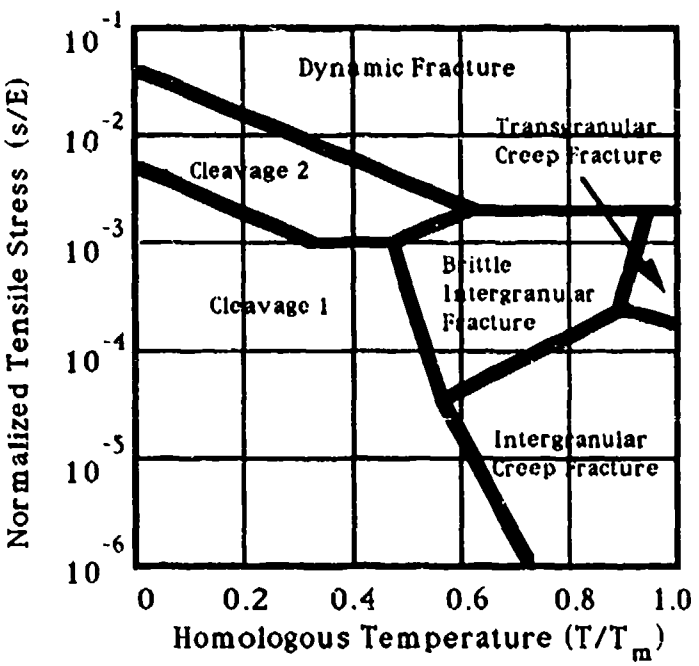

Figure 15: Fracture Mechanism Map For Alumina

(From Ashby, M.F., *Micromechanisms of Fracture in Static and Cyclic Failure*, Fracture Mechanics - Current Status, Future Prospects, Pergamon Press, 1979)

5.0 Conclusions

Microwave tube failures can be attributed mainly to three factors. Manufacturing defects, insufficient operating/handling procedures and finally, inadequate design margin between operating point and design limit are major contributors to tube failures. The objective of this study was to investigate the thermal/mechanical performance of the TWT's interaction circuit when subject to full forward and worst case reflected power. It was assumed that this TWT had not experienced any improper operating or handling procedures.

Results from the finite element analyses indicated that the interaction circuit's mechanical design is sound and would not exhibit any mechanical failure mechanisms as long as there were no pre-existing cracks or flaws in the helix or support rods. If thorough inspection techniques are used on these components prior to TWT assembly, there would be no mechanical failures associated with the interaction circuit.

The results of this study have demonstrated that finite element element analysis is a valuable tool that can be used to assess interaction circuit thermal/mechanical performance. The heat transfer capability of the slow wave structure is one of the most important factors that limit the output power capability of helix TWT's. Tube designers must be able to examine thermal behavior of the circuit, especially the dielectric support rods which play a critical role in removing heat from the helix [4]. By employing finite element techniques, tube designers can be able to estimate the feasibility of a projected design by predicting influences of various physical and geometrical parameters of the interaction circuit on helix temperatures for various power dissipations.

Several significant objectives have been accomplished in this effort. The results of this effort have significantly extended the fundamental understanding of the material behavior within helix interaction circuits subjected to forward and worst case reflected power. Secondly, a cost effective analysis technique has been developed for modeling helix interaction circuits and analytically predicting their dynamic behavior while operating in their system environments. Finally, a technique has

been developed to determine the short and long-term effects on materials used within TWT interaction circuits and the long-term mechanical structural instabilities that exist within a TWT's vacuum envelope.

6.0 References

1. *Aerospace Structural Metals Handbook*, 1991 Edition, CINDAS/Purdue University, West Lafayette, IN.

2. Ashby, M.F., *Micromechanisms of Fracture in Static and Cyclic Failure*, Fracture Mechanics - Current Status, Future Prospects, Pergamon Press, 1979, pp 1-24.

3. Bartos, K.A., Fite, E.B., Shalkhauser, K.A., Sharp, G.R., *A Three-Dimensional Finite-Element Thermal/Mechanical Analytical Technique for High-Performance Traveling Wave Tubes*, NASA Technical Paper 3081, June 1991.

4. Bukhanovskii, V.V., *Characteristics of Strength and Plasticity of Tungsten and Tungsten-Base Alloys*, Soviet Powder Metallurgy and Metal Ceramics, Vol. 2418, August 1985, pp 652-657.

5. Collins, J.A., *Failure of Materials in Mechanical Design*, John Wiley, New York, 1981, pp 128-130.

6. Crivello, R., Grow, R.W., *Thermal Analysis of PPM-Focused Rod-Supported TWT Helix Structures*, IEEE Transactions on Electronic Devices, Vol. 35, No. 10, October 1988.

7. Gilmour, A.S. Jr., *Microwave Tubes*, Artech House, Dedham, MA, 1986, pp 241-261.

8. Hughes Aircraft Company, *Hughes TWT and TWTA Handbook.*

9. Hughes Aircraft Company, *Reliability Design Criteria For High Power Tubes*, RADC-TR-88-304, Vol. 1, Part A, February 1989, pp 2-75 - 2-127. (B132722)

10. Incropera, F.P., DeWitt, D.P., *Fundamentals of Heat and Mass Transfer*, John Wiley, New York, 1985, pp 755-759.

11. Shames, I.H., *Introduction To Solid Mechanics*, Prentice Hall, Englewood Cliffs, N.J., 1975, pp 371-384.

12. Southern Research Institute, *Report on the Mechanical and Thermal Properties of Tungsten and TZM Sheet Produced in The Refractory Metal Sheet Rolling Program*, Contract No. N600(19)-59530, August 1966.

13. Yamada, D.K., *918H TWT Output Circuit Thermal Analysis*, Hughes Aircraft Company, Electron Dynamics Division, May 1983.

☆U.S. GOVERNMENT PRINTING OFFICE 1993-710-093-60180